

# Radiation pressure driven vibrational modes in ultra-high-Q silica microspheres

R. Ma, A. Schliesser, P. Del'Haye, A. Dabirian, T. J. Kippenberg

Max-Planck-Institut für Quantenoptik, Hans-Kopfermann-Str. 1, 85748 Garching, Germany

Quantitative measurements of the vibrational eigenmodes in ultra-high-Q silica microspheres are reported. The modes are efficiently excited via radiation-pressure induced dynamical back-action of light confined in the optical whispering-gallery modes of the microspheres (i.e. via the parametric oscillation instability). Two families of modes are studied and their frequency dependence on sphere size investigated. The measured frequencies are in good agreement both with Lamb's theory and numerical finite element simulation and are found to be proportional to the sphere's inverse diameter.

Silica microcavities[1] such as microspheres[2] or microtoroids[3] possess ultra-high-Q optical whispering gallery modes (WGMs), while simultaneously exhibiting mechanical modes which lie typically in the radio frequency range. Owing to the resonant buildup of light within these cavities the effect of radiation pressure is enhanced, leading to mutual coupling between the mechanical and optical modes, as first predicted by Braginsky in the context of the Laser Interferometer Gravitational Wave Observatory, LIGO[4]. When entering the regime where the photon lifetime is comparable to the mechanical oscillation period and the cavity is pumped with a laser whose frequency slightly exceeds the WGM resonance (i.e. blue-detuned excitation), this mutual coupling gives rise to a parametric oscillation instability[4] which is characterized by regenerative mechanical oscillation of the mechanical eigenmodes. This phenomenon has been first reported in toroid microcavities [5, 6, 7]. On the other hand, red-detuned light can induce cooling of the mechanical mode, as recently reported[8, 9, 10]. In this letter, parametric oscillation instability in ultra-high-Q silica microspheres is observed and the mechanical resonant frequencies and mode patterns studied. In contrast to earlier studies of acoustic modes of nanospheres[11, 12] using Raman or Brillouin scattering from ensembles, the present method allows measurement of the mechanical modes of single microspheres in a larger diameter regime (35-110  $\mu\text{m}$  in our case). Furthermore, the mechanical Q-factors are determined.

Ultra high-Q ( $Q > 10^8$ ) silica microspheres are fabricated by melting the tip of a single mode optical fiber with a  $\text{CO}_2$  laser ( $\lambda = 10.6 \mu\text{m}$ ). Due to the strong absorption of silica around  $10.6 \mu\text{m}$ , surface tension induces highly symmetric silica spheres with a near-atomically smooth surface[13]. The sphere is held by a thin fiber stem (cf. Fig. 1 inset). The WGM are excited with high ideality[14] by evanescent coupling via a tapered optical fiber [15] using a 1550-nm tunable external cavity diode laser as pump source. Owing to the high finesse (approximately  $10^5$ ), the large optical energy stored in the microcavity exerts a force on the cavity sidewalls due to radiation pressure. This force can give rise to regeneratively driven mechanical oscillations if photon lifetime is similar to the inverse acoustic resonance frequency[5, 6]. In essence, the radial force exerted by radiation pres-

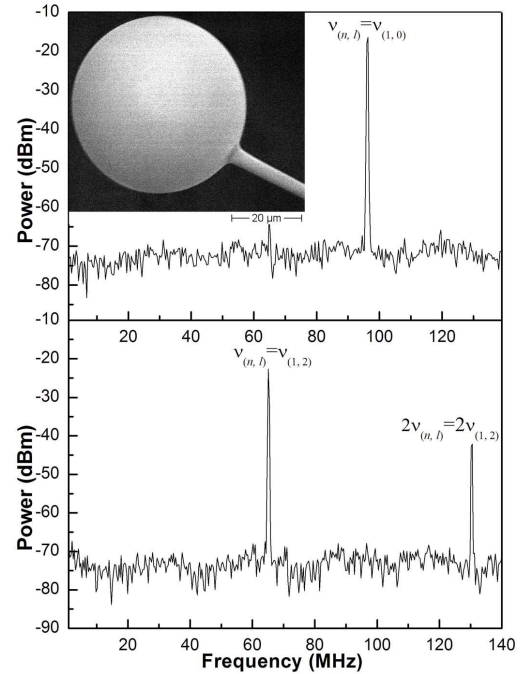


FIG. 1: Spectrum of the transmitted optical laser of the fiber taper when coupled to a silica microsphere with a diameter of  $49 \mu\text{m}$ . Two families of spheroidal mechanical modes could be driven regeneratively. Specifically, the modes are identified as  $\nu_{(1,2)}$  (a quadrupole mode) and  $\nu_{(1,0)}$  (a radial breathing mode). The launched power in this experiment was 600 micro-Watts and was sufficient to exceed the threshold for parametric oscillation instability. The inset shows the SEM image of the microsphere.

sure takes the cavity out of resonance by deformation of the cavity wall which causes subsequently a reduction in the radiation pressure force. The whole process resumes upon the restoration of the original shape of the cavity, leading to a periodic motion of the cavity. In this way, modes with radial deformation can be excited which modify the path length of the optical wave and therefore affect the magnitude of the radiation force. In

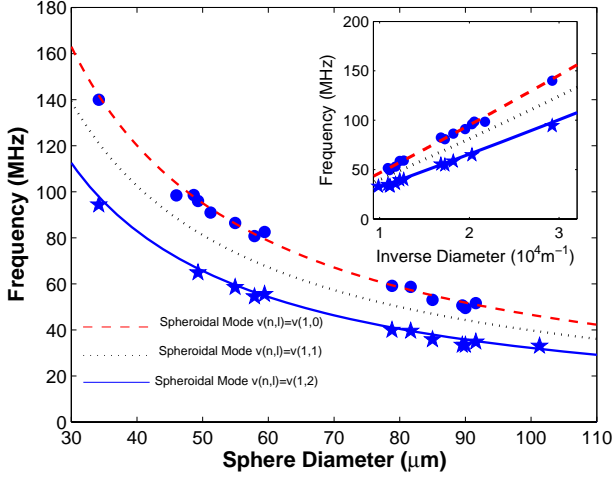


FIG. 2: Experimentally measured frequencies of the spheroidal modes, with stars denoting the  $\nu_{(1,2)}$  mode and dots denoting the  $\nu_{(1,0)}$  mode. Numerically calculated eigenfrequencies of these modes are shown in blue solid line ( $\nu_{(1,2)}$ ) and red dashed line ( $\nu_{(1,0)}$ ). Spheroidal mode  $\nu_{(1,1)}$  with the frequencies lie between  $\nu_{(1,2)}$  and  $\nu_{(1,0)}$ , which is not experimentally observed, is also presented in black dotted line. The inset shows the relationship between the frequencies of the eigenmodes and the inverse diameter of the silica microspheres.

the present experiments the threshold for the parametric instability was in the range of typically 100 micro-Watts. The driven mechanical oscillations causes the appearance of motional sidebands (and their harmonics) which can be readily detected in the spectrum of the transmitted laser light using an electronic spectrum analyzer. Fig. 1. shows a typical spectrum of the transmission, showing regenerative oscillations of two different mechanical eigenmodes of the same sphere under different taper loading conditions. By changing the taper loading (and hence the optical Q) the value of the oscillation threshold of the two modes crosses, thereby causes a switching from the low- to a high frequency mode as coupling strength increases and the optical linewidth decreases, in agreement with the theoretical predictions[16]. To identify the mode families, the vibrational frequencies of the two lowest lying mechanical frequencies were recorded as a function of size. While observable in principle, light-induced modifications of the mechanical modes' dynamical properties[10], in particular shifts in the mechanical resonance frequency, are considered to be small (relative frequency shift typically  $< 0.1\%$ ) and are neglected in this letter. The result of this study is shown in Fig. 2. As evident, the spheres mechanical frequencies are inversely proportional to the sphere diameter.

Next, the observed modes were identified by numerical studies. Since the fabricated silica microspheres exhibited no observable eccentricity under SEM imaging (see the inset of Fig. 1), and the diameter ratio of the stem holding the sphere and the sphere itself is on the

order of 0.1, the sphere can be considered as almost free; hence it is a judicious choice to adopt the stress-free boundary condition. Studies on the nature of the fundamental modes of vibration for small elastic spheres with free-surface boundary condition are well known. The first well-established theory was formulated by Lamb, with two types of modes predicted, the spheroidal and torsional modes[17]. The equation describing the wave propagation in a homogeneous elastic body with free surface can be written as[18],

$$\rho \ddot{\mathbf{u}} = (\lambda + 2\mu) \nabla(\nabla \cdot \mathbf{u}) - \mu \nabla \times (\nabla \times \mathbf{u}) \quad (1)$$

where  $\mathbf{u}$  is the displacement vector,  $\rho$  is the mass density, and  $\lambda$  and  $\mu$  are Lamé constants. Here  $\lambda \equiv \frac{\sigma E}{(1+\sigma)(1-2\sigma)}$ , and  $\mu \equiv \frac{E}{2(1+\sigma)}$ , with  $E$  denoting the Young's modulus and  $\sigma$  the Poisson ratio of the material. Eq. (1) can be solved by introducing a scalar potential  $\phi_0$  and two vector potentials  $\Phi_1 = (r\phi_1, 0, 0)$  and  $\Phi_2 = (r\phi_2, 0, 0)$  with  $\mathbf{u} = \nabla\phi_0 + \nabla \times \Phi_1 + \nabla \times \nabla \times \Phi_2$ . Then the general solutions of the equations resulting from (1) are written as

$$\phi_2 = \sum_{\ell, m} A_i^{(\ell, m)} j_\ell\left(\frac{2\pi\nu_{n, \ell, m} \mathbf{r}}{V_1}\right) Y_\ell^m(\theta, \Psi) e^{-2\pi i \nu_{n, \ell, m} t} \quad (2)$$

where  $j_\ell$  is the spherical Bessel function and  $Y_\ell^m$  is the spherical harmonic function and  $V_0$  is the longitudinal sound velocity and  $V_1 = V_2$  are the transverse sound velocities. An angular momentum mode number  $\ell$  ( $\ell = 0, 1, 2, \dots$ ), an azimuthal mode number  $m$  ( $-\ell \leq m \leq \ell$ ) and a radial mode number  $n$  ( $n = 1, 2, \dots$ ) are used to characterize the acoustic modes, where  $n = 1$  corresponds to the surface mode and  $n \geq 2$  to inner modes and  $\nu_{n, \ell, m}$  denotes the frequency of the vibration characterized by the mode numbers  $(n, \ell, m)$ . It is noteworthy that a spheroidal mode with angular momentum  $\ell$ , is  $(2\ell + 1)$ -fold degenerate, hence in Fig. 1 we use  $(n, \ell)$  instead of  $(n, \ell, m)$  to assign the eigenfrequencies.

Two classes of modes are derived when applying the free boundary condition[18]. One of them is the torsional vibration which induces only shear stress without volume change, and no radial displacement takes place in these modes. Thus these modes cannot be excited using radiation pressure which relies on a change in the optical path length. In contrast, the class of mode in which volume change is present is referred to as spheroidal modes. According to Lambs theory the  $\ell = 0$  spheroidal mode eigenvalue equation is written as

$$\frac{\tan(hR)}{hR} - \frac{1}{1 - \frac{1}{4}(k^2/h^2)h^2 R^2} = 0 \quad (3)$$

where  $k = 2\pi\nu/V_1$ ,  $h = 2\pi\nu/V_0$ ,  $R$  is the radius of the sphere,  $V_0 = \sqrt{(\lambda + 2\mu)/\rho}$ , and  $V_1 = V_2 = \sqrt{\mu/\rho}$ . Other eigenvalue equations for torsional modes and  $\ell > 0$  spheroidal modes are contained in Ref.[17]. Next, the resonant frequencies of the lowest frequencies (i.e.  $n = 1, \ell = 0, 1, 2$ ) were numerically calculated as a function of

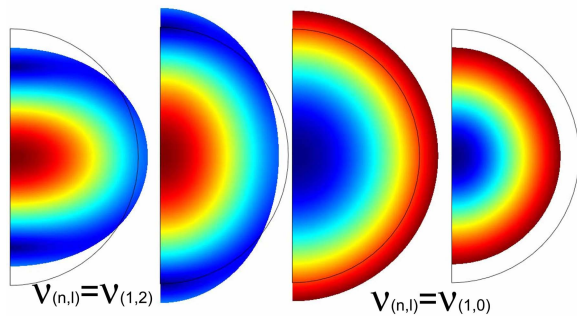


FIG. 3: Finite element modeling of three spheroidal modes  $\nu_{(1,2)}$  (left) and  $\nu_{(1,0)}$  (right) of a silica microsphere with its von Mises stress (color coded) and deformed shape (greatly exaggerated for clarity).

sphere size (compare Fig. 2, solid lines). The eigenvalues versus the inverse of the diameters are shown in the inset. As seen from Fig. 2 the measured data fit very well to the theoretical prediction based on the  $\nu_{(1,0)}$  (radial breathing) and  $\nu_{(1,2)}$  (quadrupole) mode, and reveals that the eigen-frequencies of the microspheres have linear dependence on the inverse microsphere diameter.

We note that the sphere's eccentricity can lift the  $(2\ell + 1)$ -fold degeneracy in the mode number  $m$  of the  $\nu_{(1,2)}$  mode[19], which in the experiments was not observed owing to the high degree of symmetry of the microspheres.

It is worth pointing out that  $\ell = 1$  spheroidal mode has the eigenfrequency lying between  $\ell = 0$  and  $\ell = 2$  spheroidal modes (Fig. 2); however, it is not observed in the experiment since  $\ell = 1$  spheroidal mode result in a vanishing path length change around the optical whispering gallery mode trajectory such that the mutual coupling of optical and mechanical mode vanishes.

To gain a more complete understanding of the mechanical modes, the numerical studies were complemented with finite element simulations of the stress and strain fields. Using axial symmetric finite element modeling, the mode families  $\nu_{(1,0)}$  and  $\nu_{(1,2)}$  were calculated and excellent agreement found with the numerical solution of the preceding section. In the simulation, a Young's modulus of  $73.1 \times 10^9$  Pa, a Poisson ratio of 0.17 and a density of the microsphere of  $2.203 \times 10^3$  kg/m<sup>3</sup> is used (Corresponding to  $\lambda = 16.09 \times 10^9$  Pa and  $\mu = 31.24 \times 10^9$  Pa). The longitudinal and transverse sound velocities are 5972 m/s and 3755 m/s, respectively. Fig. 3 depicts the deformed shape and von Mises stress, as obtained from finite element simulations of two spheroidal modes with the lowest frequencies. The stresses are greatly exaggerated for clarity.

To determine the mechanical dissipation of the vibrational modes, the mechanical quality factor of the sphere modes were measured in the sub-threshold regime (in a purged nitrogen environment). For this measurement the laser power was adjusted to a level far below the threshold of the mechanical oscillation. In addition, the mechan-

ical Q factor was measured for both blue-detuning (i.e. where the radiation pressure decreases the mechanical dissipation, causing mechanical amplification) and red-detuning (where the radiation pressure causes the mechanical damping to be increased, leading to cooling). Both values coincided closely, and yielded Q-values of up to 7000 for the radial breathing mode. Note that the Q was difficult to measure for the  $\ell = 2$  mode owing to the 5-fold degeneracy of the mode which precludes fitting of the spectrum with a single oscillator function.

In conclusion, spheroidal acoustic modes in silica microspheres driven by radiation pressure induced parametric oscillation instability are reported. The observed vibrational modes are indentified as spheroidal modes whose frequencies agree well with Lamb's theory and numerical simulation and exhibit a linear dependence on the inverse of the sphere diameters.

### A. Acknowledgements

We thank Prof. Dr. Grundler and Dr. Berberich in the physics department of Technical University of Munich for providing access to the SEM. This work was funded via a Max Planck Independent Junior Research Group grant and a Marie Curie International Reintegration, a Marie Curie Excellence Grant (RG-UHQ) and the NIM Initiative.

- 
- [1] K. J. Vahala, *Nature* **424**, 839 (2003).
- [2] V. B. Braginskii and V. S. Ilchenko, *Doklady Akademii Nauk Sssr* **293**, 1358 (1987).
- [3] D. K. Armani, T. J. Kippenberg, S. M. Spillane, and K. J. Vahala, *Nature* **421**, 925 (2003).
- [4] V. B. Braginsky, S. E. Strigin, and S. P. Vyatchanin, *Physics Letters A* **287**, 331 (2001).
- [5] H. Rokhsari, T. J. Kippenberg, T. Carmon, and K. J. Vahala, *Optics Express* **13**, 5293 (2005).
- [6] T. J. Kippenberg, H. Rokhsari, T. Carmon, A. Scherer, and K. J. Vahala, *Physical Review Letters* **95**, 033901 (2005).
- [7] T. Carmon, H. Rokhsari, L. Yang, T. J. Kippenberg, and K. J. Vahala, *Physical Review Letters* **94** (2005).
- [8] S. Gigan, H. R. Bohm, M. Paternostro, F. Blaser, G. Langer, J. B. Hertzberg, K. C. Schwab, D. Bauerle, M. Aspelmeyer, and A. Zeilinger, *Nature* **444**, 67 (2006).
- [9] O. Arcizet, P. F. Cohadon, T. Briant, M. Pinard, and A. Heidmann, *Nature* **444**, 71 (2006).
- [10] A. Schliesser, P. Del'Haye, N. Nooshi, K. J. Vahala, and T. J. Kippenberg, *Physical Review Letters* **97** (2006).
- [11] H. S. Lim, M. H. Kuok, S. C. Ng, and Z. K. Wang, *Applied Physics Letters* **84**, 4182 (2004).
- [12] M. H. Kuok, H. S. Lim, S. C. Ng, N. N. Liu, and Z. K. Wang, *Physical Review Letters* **90** (2003).
- [13] V. B. Braginskii, V. S. Ilchenko, and M. L. Gorodetskii, *Uspekhi Fizicheskikh Nauk* **160**, 157 (1990).
- [14] S. M. Spillane, T. J. Kippenberg, O. J. Painter, and K. J. Vahala, *Physical Review Letters* **91**, art. no. (2003).
- [15] M. Cai, O. Painter, and K. J. Vahala, *Physical Review Letters* **85**, 74 (2000).
- [16] H. Rokhsari, I. J. Kippenberg, T. Carmon, and K. J. Vahala, *Ieee Journal of Selected Topics in Quantum Electronics* **12**, 96 (2006).
- [17] H. Lamb, *Proc. London. Math. Soc.* p. 189 (1884).
- [18] N. Nishiguchi and T. Sakuma, *Solid State Communications* **38**, 1073 (1981).
- [19] A. Tamura, K. Higeta, and T. Ichinokawa, *Journal of Physics C-Solid State Physics* **15**, 4975 (1982).